

Analogue Radio-Over-Fiber Fronthaul with UDWDM-based Delay Dissemination for Photonic-Assisted RF Beam Steering

Dinka Milovančev, Nemanja Vokić, David Löschenbrand, Thomas Zemen, and Bernhard Schrenk

AIT Austrian Institute of Technology, Center for Digital Safety&Security / Security & Communication Technologies, 1210 Vienna, Austria.

Author e-mail address: bernhard.schrenk@ait.ac.at

We integrate beam steering in a coherent ultra-dense WDM fronthaul to steer the beam of a 1×3 phased-array remote radio head. Deflected OFDM radio signal transmission at a low error vector magnitude of 3.4% is experimentally demonstrated in virtue of low-complexity coherent receivers.

1. Introduction

Fifth-generation (5G) cellular networks build on an optical fiber infrastructure to support cloud-based remote access networks (C-RAN) [1]. For this mobile fronthaul, the translation from the optical to the electrical domain must ensure good signal integrity, thus digital radio-over-fiber (RoF) transmission is commonly used [2, 3]. However, the transmission of digitized radio signals at the optical layer requires high-resolution ADC/DAC functions at each antenna location. This undermines the cost- and energy-efficiency of C-RANs, in which centralized digital functions are desired. For this reason, analog RoF transmission schemes are of high interest as they aim to omit ADC/DAC and digital signal processing (DSP) functions at the antenna sites [4, 5]. Moreover, the evolution towards millimeter-wave technology offers high data rates delivered to the user while at the same time interference is avoided. However, the associated beamforming functions are often subject to high complexity.

In this work we demonstrate an analogue coherent optical fronthaul that integrates true time delay (TTD) functionality for the purpose of RF beam steering. The remote radio head (RRH) optics build on a commercial EML device to enable reception for ultra-dense WDM (UDWDM) [6], which together with delay dissemination at the fronthaul allows us to steer the beam of a 1×3 antenna configuration at low error vector magnitude (EVM) of 3.4%.

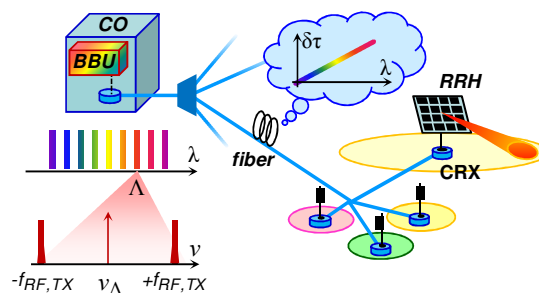


Fig. 1. Analogue UDWDM fronthaul with true time delay dissemination and coherent receivers at the RRHs.

2. UDWDM RAN with integrated beam steering

The mobile fronthaul that expands analogue RoF transmission by true time delay dissemination is presented in Fig. 1. Centralized RF management at the central office (CO) builds on a filterless UDWDM broadcast-and-select methodology as it is known from wired optical access networks.[7] The RRHs in the field, which may incorporate phased-array antenna functionality, then select their optical target channel based on the corresponding RoF signal and delay value. The joint channel/delay selection is facilitated by means of coherent receivers (CRX). The pivotal aspect of implementing the UDWDM fronthaul is the realization of a low-complexity CRX that satisfies the requirements of analogue RoF transmission. Towards this direction, a coherent homodyne receiver based on a

transistor-outline EML is being applied, as introduced in our previous works [8, 9]. In such a receiver, frequency offset and phase noise are mitigated by means of injection locking. Figure 2(a) details the homodyne CRX architecture for a multi-element RRH. The transmitted radio signal at the wavelength $\Lambda^{(i)}$ is detected by the electroabsorption (EAM) section of EML which serves as a photodetector in which the local oscillator (LO) provided by the DFB section beats the radio signal. As demonstrated earlier [8], the wavelengths of LO and the RoF input signal can be precisely matched in virtue of injection locking. This requires that both optical carrier frequencies fall within the locking range of typically 500 MHz for an input power of -22 dBm. Initial tuning of the LO through adjustment of either DFB bias current or temperature ensures this condition. As a result of homodyne detection, there are no DSP functions required as they are common for standard coherent receiver schemes [10]. Homodyne reception further allows RoF transmission with much simpler double-sideband modulation (Fig. 1).

It shall be further stressed that polarization independent operation can be achieved if a tandem-EML configuration is used [11]; this aspect will not be demonstrated in this work due to limited number of available EMLs.

The ease of coherent reception is here exploited for selecting not only a RoF channel, but also to select a delay value for the purpose of beam steering. Although a variety of TTD implementations have been proposed [12-15], the re-use of a dispersive transmission medium such as the standard single-mode fiber (SMF) allows for a simple delay dissemination. Since the true time delay is wavelength dependent, $\delta\tau = f(\lambda)$, the RF carrier phase shift at the antenna element after analogue RoF transmission is simply determined by tuning the corresponding EML CRX to desired UDWDM channel. Compared to previous demonstrations building on fiber dispersion [16, 17], no fixed demultiplexing filters are required anymore. The filterless UDWDM scheme therefore contributes to the scalability and flexibility of the TTD architecture.

The expected wavelength-dependent time delay was investigated by measuring the phase shift of a 3.5 GHz tone within the EML tuning range. Figure 2b shows that phase slope in the case of propagation through SMF is $-302^\circ/\text{nm}$, whereas for the C-FBG it is $25^\circ/\text{nm}$.

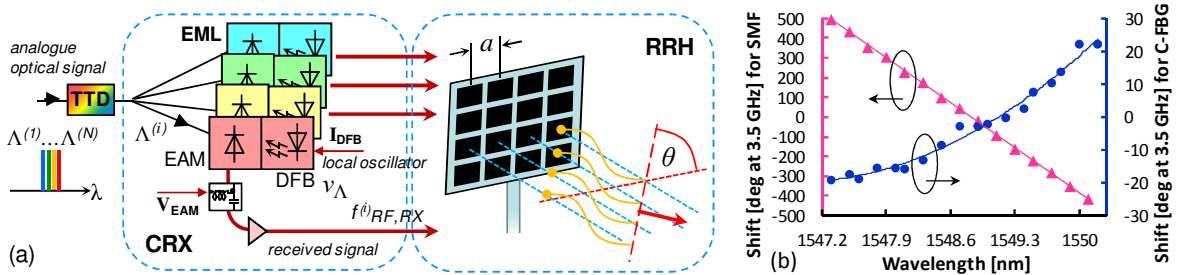


Fig. 2. (a) CRX-assisted RRH. (b) Phase shift of a 3.5 GHz signal propagating through 14.3 km of SMF (▲) and C-FBG (●).

3. Experimental setup

A comb of three closely spaced UDWDM channels around 1548 nm were double-sideband modulated by the Mach-Zehnder modulator (Fig. 3). An OFDM radio signal with a bandwidth of 125 MHz at a carrier frequency of 3.5 GHz was used in order to prove the RoF concept. The modulated comb was then amplified by an EDFA and launched at an OSNR of 37 dB / 0.1 nm for transmission over a 14.3 km long SMF feeder. Each of transmitted lines ($\nu_1 \dots \nu_3$) experiences a different time delay as it propagates along SMF. Additional time delay customization can be achieved through insertion of a chirped fiber Bragg grating (C-FBG). A colorless 1×3 split delivers the comb with an optical power of -18.7 dBm/λ to the three polarization-controlled EMLs receivers.

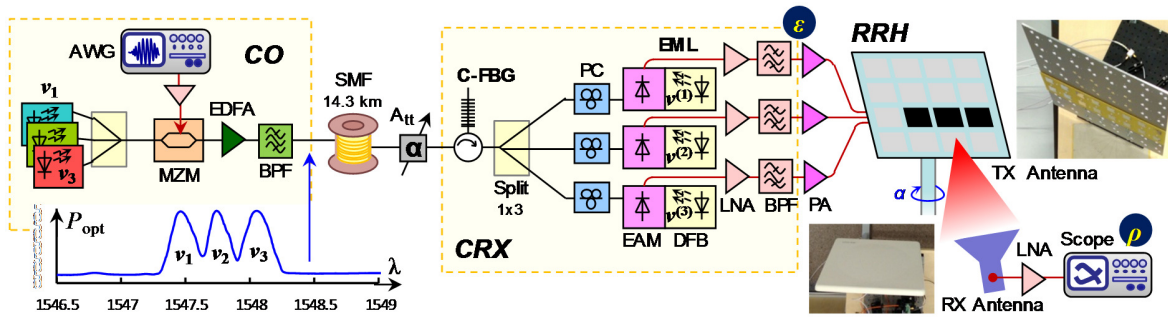


Fig. 3. Experimental setup of the analogue coherent optical fronthaul with integrated beamforming.

Each of the EML outputs is amplified, bandpass filtered and fed to the corresponding element of a 1×3 patch antenna. The EMLs can be locked on the same or on different UDWDM channels, resulting in the change of the RF carrier phase among the antenna elements. The transmitted antenna beam was received by a high-directivity (18 dBi gain) antenna. In this way the beam characteristics and the OFDM transmission performance has been obtained.

4. Experimental results

The beam steering capabilities were investigated by locking all three EMLs on the same optical comb line ν_2 , which was modulated solely by the RF carrier of the OFDM radio signal. As Fig. 4(a) shows, there is no phase difference between the three detected RF carriers, which are subsequently fed to antenna elements. By contrast, when locking the EMLs each on different ν_i , there is a phase shift of $\varphi = 73^\circ$ between the respective RF signals ($\nu_1 \dots \nu_3$), see Fig. 5(b). This phase shift agrees well with the expected phase shift of 79° for the used channel spacing of 0.29 nm. The phase shift, i.e. time delay $\delta\tau$ among the RF carriers, is translated to a beam steering angle $\theta = \arcsin(c \delta\tau / a)$, where c is the speed of light and a is the physical spacing between antenna elements of $0.6 \lambda_{RF}$. According to the above equation, the expected beam steering angle is 19.8° .

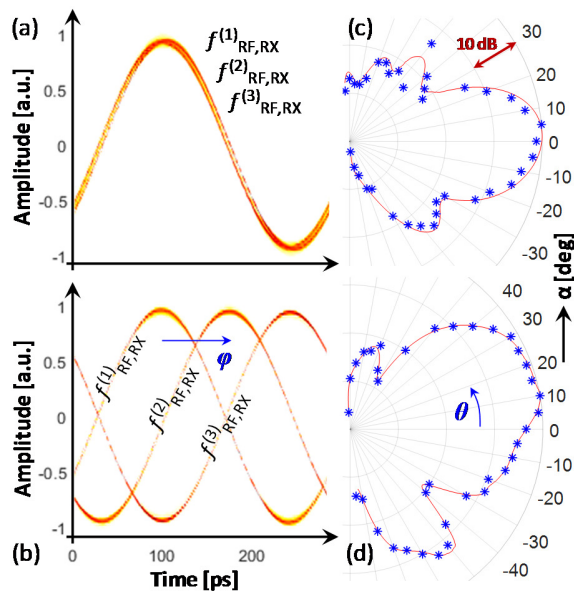


Fig. 4. RF carrier signals and beam profiles when the EML-based CRXs are locked on (a,c) the same UDWDM channel ν_2 and (b,d) different UDWDM channels $\nu_1 \dots \nu_3$.

For the experimental verification of the beam steering, the receive antenna output was monitored on the spectrum analyzer. The transmit antenna was rotated (α in Fig. 3) while the high directivity receive antenna was fixed with

respect to its orientation. Figure 4(c) shows the measured beam pattern when all EMLs are locked on the same comb line, leading to $\varphi = 0^\circ$ and resulting in a peak value in the beam profile at $\alpha = 0$. For the case of locking to the three comb lines, the resulting phase shift of $\varphi = 73^\circ$ leads to a rotation of $\sim 20^\circ$ in the beam profile, as reported in Fig. 4(d). This agrees well with the predicted beam steering value.

The quality of radio signal transmission was evaluated by measuring the EVM of a 16-QAM OFDM radio signal after coherent detection with the EML (ε) and after propagation over the RF path between 1x3 transmit and receive antennas (ρ). Figure 5(a) presents the corresponding EVM performance for its 128 OFDM sub-carriers. The average EVM is 3.37% and its low value is also evident from the clearly distinguishable constellation points. There is no penalty due to coherent optical RoF transmission and its integrated beam steering.

The received OFDM spectrum, included as inset in Fig. 5(a), features a clear pilot (π) at the 3.5 GHz RF carrier frequency in virtue of the coherent homodyne detection through the EML.

Figure 5(b) reports the EVM when the angle α of the transmit antenna is being altered. If there is no beam steering ($\varphi = 0$ and thus $\theta = 0$), the minimum EVM is obtained at $\alpha = 0$. The EVM worsens to 4.6% for a transmit antenna rotation of $\alpha = -20^\circ$. With present beam steering at $\varphi = 73^\circ$ as introduced earlier, the minimum EVM of 3.35% now shifts and is found for a transmit antenna rotation of $\alpha = 20^\circ$. In this case the original face-to-face alignment of transmit and receive antennas ($\alpha = 0$) leads to an increased EVM of 5.68%. This confirms the photonic beam steering at the optical fronthaul.

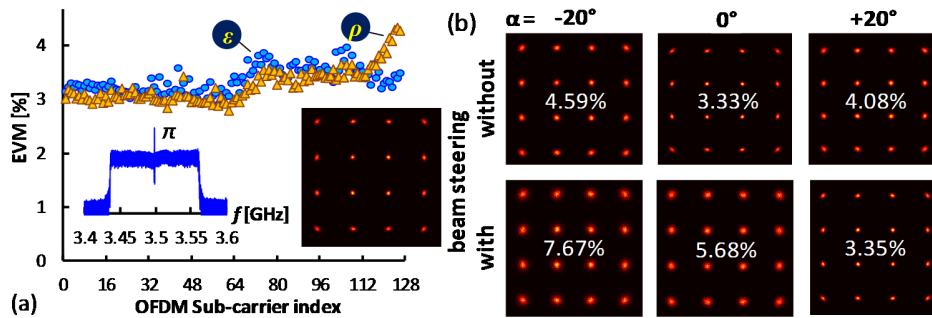


Fig. 5. (a) EVM performance over optical fronthaul (ε) and including the RF propagation (ρ). The inset shows the received radio signal at the EML output. (b) EVM after RF propagation as function of the transmit antenna angle α .

4. Conclusion

We demonstrated a coherent optical mobile fronthaul with integrated beam steering based on a UDWDM delay dissemination method. Steering of a 3.5 GHz OFDM radio signal by 20° has been obtained at a low 3.4% EVM, which confirms the correct operation. The obtained results agree well with the expectations.

5. Acknowledgement

This work was supported by the European Research Council under grant No 804769 and the Austrian FFG project TRITON (858697).

6. References

- [1] I.A. Alimi, A.L. Teixeira, and P.P. Monteiro, "Toward an Efficient C-RAN Optical Fronthaul for the Future Networks: A Tutorial on Technologies, Requirements, Challenges, and Solutions," *IEEE Comm. Surveys & Tutorials*, vol. 20, no. 1, pp. 708-769, 2018.
- [2] X. Liu, H. Zeng, N. Chand, and F. Effenberger, "Efficient Mobile Fronthaul via DSP-based Channel Aggregation," *IEEE/OSA J. Lightwave Technol.*, vol. 34, no. 6, pp. 1556-1564, Mar. 2016.
- [3] T. Pfeiffer, "Next Generation Mobile Fronthaul and Midhaul Architectures," *IEEE/OSA J. Opt. Comm. Netw.*, vol. 7, no. 11, pp. B38-B45, 2015.
- [4] H.N. Parajuli et al., "Experimental demonstration of multi-Gbps multi sub-bands FBMC transmission in mm-wave radio over a fiber system," *OSA Opt. Expr.*, vol. 26, no. 6, pp. 7306-7312, 2018.

- [5] N. Argyris et al., "A 5G mmWave Fiber-Wireless IFoF Analog Mobile Fronthaul Link With up to 24-Gb/s Multiband Wireless Capacity," *IEEE/OSA J. Lightwave Technol.*, vol. 37, no. 12, pp. 2883-2891, Feb. 2020.
- [6] B. Schrenk, "The EML as Analogue Radio-over-Fiber Transceiver – a Coherent Homodyne Approach," *IEEE/OSA J. Lightwave Technol.*, vol. 37, no. 12, pp. 2866-2872, Jun. 2019.
- [7] H. Rohde et al., "Trials of a Coherent UDWDM PON Over Field-Deployed Fiber: Real-Time LTE Backhauling, Legacy and 100G Coexistence," *IEEE/OSA J. Lightwave Technol.*, vol. 33, no. 8, pp. 1644-1649, Apr. 2015
- [8] B. Schrenk, "Injection-Locked Coherent Reception Through Externally Modulated Laser," *IEEE J. Sel. Topics in Quantum Electron.*, vol. 24, no. 2, p. 3900207, Mar. 2018.
- [9] B. Schrenk, and F. Karinou, "A Coherent Homodyne TO-Can Transceiver as Simple as an EML," *IEEE/OSA J. Lightwave Technol.*, vol. 37, no. 2, pp. 555-561, Jan. 2019.
- [10] S.J. Savory, "Digital Coherent Optical Receivers: Algorithms and Subsystems," *IEEE J. Sel. Topics in Quantum Electron.*, vol. 16, no. 5, pp. 1164-1179, Sep. 2010.
- [11] B. Schrenk, and F. Karinou, "Simple Laser Transmitter Pair as Polarization-Independent Coherent Homodyne Detector," *OSA Opt. Expr.*, vol. 27, no. 10, pp. 13942-13950, May 2019.
- [12] Y. Liu, B. Isaac, J. Kalkavage, E. Adles, T. Clark, and J. Klamkin, "93-GHz Signal Beam Steering with True Time Delayed Integrated Optical Beamforming Network," in *Proc. Opt. Fib. Comm. Conf. (OFC)*, San Diego, United States, Mar. 2019, Th1C.5.
- [13] X. Wang, L. Zhou, R. Li, J. Xie, L. Lu, K. Wu, and J. Chen, "Continuously tunable ultra-thin silicon waveguide optical delay line," *OSA Optica*, vol. 4, no. 5, pp. 507-515, May 2017.
- [14] R. Bonjour et al., "Plasmonic phased array feeder enabling ultrafast beam steering at millimeter waves," *OSA Opt. Expr.*, vol. 24, no. 22, pp. 25608-25618, Oct. 2016.
- [15] G. Wang et al., "Continuously tunable true-time delay lines based on a one-dimensional grating waveguide for beam steering in phased array antennas," *Appl. Opt.*, vol. 57, no. 18, pp. 4998-5003, Jun. 2018.
- [16] H.B. Jeon, J.W. Jeong, and H. Lee, "Optical True Time-Delay for Phased-Array Antenna System Using Dispersion Compensating Module and a Multi-wavelength Fiber Laser," in *Proc. Opto-Electron. and Comm. Conf. (OECC)*, Busan, Korea, Jul 2012, P1-40.
- [17] D.B. Hunter, M.E. Parker, and J.L. Dexter, "Demonstration of a Continuously Variable True-Time Delay Beamformer Using a Multichannel Chirped Fiber Grating," *IEEE Trans. Microwave Theory and Tech.*, vol. 54, no. 2, pp. 861-867, Feb. 2006.